Contactless electroreflectance and theoretical studies of band gap and spin-orbit splitting in $InP_{1-x}Bi_x$ dilute bismide with $x \leq 0.034$

J. Kopaczek,[1] R. Kudrawiec,[1,a)] M. P. Polak,[1] P. Scharoch,[1] M. Birkett,[2] T. D. Veal,[2] K. Wang,[3] Y. Gu,[3] Q. Gong,[3] and S. Wang[3,4]

[1]*Institute of Physics, Wrocław University of Technology, Wybrzeże Wyspiańskiego 27, 50-370 Wrocław, Poland*

[2]*Stephenson Institute for Renewable Energy and Department of Physics, School of Physical Sciences, University of Liverpool, Liverpool L69 7ZF, United Kingdom*

[3]*State Key Laboratory of Functional Materials for Informatics, Shanghai Institute of Microsystem and Information Technology, Chinese Academy of Sciences, Shanghai 200050, China*

[4]*Department of Microtechnology and Nanoscience, Chalmers University of Technology, Gothenburg 41296, Sweden*

(Received 17 October 2014; accepted 19 November 2014; published online 2 December 2014)

Contactless electroreflectance is applied to study the band gap (E_0) and spin-orbit splitting (Δ_{SO}) in $InP_{1-x}Bi_x$ alloys with $0 < x \leq 0.034$. The E_0 transition shifts to longer wavelengths very significantly (−83 meV/% Bi), while the $E_0 + \Delta_{SO}$ transition shifts very weakly (−13 meV/% Bi) with the rise of Bi concentration. These changes in energies of optical transitions are discussed in the context of the valence band anticrossing model and *ab initio* calculations. Shifts of E_0 and $E_0 + \Delta_{SO}$ transitions, obtained within *ab-initio* calculations, are −106 and −20 meV per % Bi, respectively, which is in a good agreement with experimental results. © *2014 AIP Publishing LLC*. [http://dx.doi.org/10.1063/1.4903179]

Ga(In)AsBi alloys with a few percent of Bi atoms (commonly known as "dilute bismides"), attracted great attention in the past decade because of their interesting fundamental properties including a large bandgap reduction (~50–90 meV per percent of Bi) and a strong enhancement of the spin-orbit splitting due to the incorporation of Bi atoms.[1–5] Very similar phenomena are expected when Bi atoms are incorporated into an InP host. However, $InP_{1-x}Bi_x$ alloys have not been investigated intensively either experimentally or theoretically. Only a few reports exist on the $InP_{1-x}Bi_x$ material system[6,7] and none of these is focus on experimental studies of spin-orbit splitting in this alloy. Moreover, none of these previous reports study the band gap of $InP_{1-x}Bi_x$ alloys by electromodulation spectroscopy, i.e., contactless electroreflectance (CER) or photoreflectance. CER, due to its differential and absorption-like character, is an excellent tool to study the band gap and the spin-orbit splitting in III-V semiconductors.[5] This Letter reports the application of CER spectroscopy to study the fundamental band gap (E_0) and the spin-orbit split ($E_0 + \Delta_{SO}$) transition in $InP_{1-x}Bi_x$ alloys with $0 < x \leq 0.034$, as well *ab-inito* calculations of the band structure for this alloy.

The InPBi films were grown on (100) semi-insulating InP substrates by V90 gas source molecular beam epitaxy.[6] Elemental In, Bi, and P_2 cracked from phosphine were applied. After the surface oxide desorption of InP substrate at 524 °C, a 75-nm undoped InP buffer was grown at 474 °C. Then the growth temperature was decreased significantly for the growth of each InPBi film. The Bi/P ratio was adjusted to achieve InPBi films with various Bi compositions. The thickness of the InPBi films was kept around 430 nm. For CER measurements, the samples were placed in a capacitor with a half-transparent top electrode made from a copper-wire mesh.[5,8] To obtain absorption spectra, transmission data were recorded using a Bruker Vertex 70V Fourier transform infrared/visible spectrometer using a tungsten lamp, a Si diode detector, and a CaF_2 beam splitter. In order to determine Bi concentration in $InP_{1-x}Bi_x$ samples, careful X-ray diffraction (XRD) and Rutherford backscattering spectrometry (RBS) studies were performed.[6,7] A summary of XRD and RBS studies is given in Table I.

Figure 1 shows the room temperature CER spectra measured for $InP_{1-x}Bi_x$ samples with various Bi concentrations together with the absorption curves (grey lines) measured at the same temperature. It is clearly visible that the energy of CER resonance, which is related to E_0 transition, agrees with the energy gap determined from absorption measurements quite satisfactorily. With increasing in Bi concentration, the E_0 transition shifts to longer wavelengths, while the $E_0 + \Delta_{SO}$ transition is observed to be almost at the same energy. For the sample with the largest Bi concentration, the $E_0 + \Delta_{SO}$ transition is not visible in the CER spectrum (see Fig. 1(c)) because strong CER resonances related to the E_0 and $E_0 + \Delta_{SO}$ transitions in the InP buffer layer are observed in this spectral region. InP-related transitions are not observed in the other samples since CER spectroscopy probes the sample region near the surface where band bending modulation is strongest. For the sample with the largest Bi concentration, the band bending modulation at the surface is suppressed, probably due to the Bi droplets on the surface, and therefore the band bending is modulated more strongly at the InPBi/InP interface. Because of this, a strong signal from the InP buffer layer is observed in CER spectrum beside the signal from InPBi epi-layer. It is worth noting that a strong signal from the InP buffer layer is also observed for all InPBi samples in photoreflectance spectra (not shown

a)E-mail: robert.kudrawiec@pwr.wroc.pl

TABLE I. Summary of XRD and RBS studies of $InP_{1-x}Bi_x$ layers. $f_\parallel$ and $f_\perp$ are the parallel and perpendicular mismatch defined, respectively, as $f_\parallel = (a_\parallel^{InPBi} - a^{InP})/a^{InP}$ and $f_\perp = (a_\perp^{InPBi} - a^{InP})/a^{InP}$, where $a_\parallel^{InPBi}$ and $a_\perp^{InPBi}$ are the lattice constants of $InP_{1-x}Bi_x$ films parallel and perpendicular to the growth direction, respectively, determined from (004) and (115) ω-2θ rocking curves.

Sample No.	$f_\parallel$ (ppm)	$f_\perp$ (ppm)	Bulk mismatch (ppm)	Relaxation (%)	Bi concentration obtained from XRD study (%)	Bi concentration obtained from RBS study (%)
A	115	5100	2457	5.0	1.6	NA
B	134	5400	2610	5.6	1.7	2.4
C	1415	6500	3826	40.5	2.8	2.8
D	517	10400	5158	11.5	3.4	4.4

here) which is typical for this technique but is unprofitable in this case, since the InP-related transitions interfere spectrally with the $E_0 + \Delta_{SO}$ transition of the $InP_{1-x}Bi_x$ epi-layer. It means that CER spectroscopy is the best tool to study the spin-orbit splitting in these samples.

In order to extract energies of E_0 and $E_0 + \Delta_{SO}$ transitions, CER spectra have been analyzed as in Ref. 5. The fitted curves are shown as thick grey lines in Fig. 1 together with the moduli of CER resonances which are shown as dashed lines. Figure 2 shows energies of E_0 and $E_0 + \Delta_{SO}$ transitions for InPBi layers extracted from the fitting procedure (open triangles) together with energies of E_0 transition obtained from absorption measurements (open squares). It is clearly visible that the energy gap narrows with increasing Bi concentration. A reasonable first approximation is to say, energies of E_0 and $E_0 + \Delta_{SO}$ transitions in this alloy with low Bi concentration ($Bi \leq 3.4\%$) decrease linearly with the slope of -83 and -13 meV/% Bi, respectively. The observed reduction of bandgap upon Bi incorporation is very different than those obtained within the virtual crystal approximation (VCA) with the InBi bandgap assumed to be -1.63 eV,[9] see the thin solid line in Fig. 2. This means that the simple VCA is inappropriate for this alloy.

To further investigate the evolution of the E_0 and $E_0 + \Delta_{SO}$ transitions with Bi content, *ab initio* calculations were performed within the density functional theory (DFT) with fully relativistic pseudopotentials on a 54 atom supercell using the SC-AM approach, which has been applied to GaAsBi and GaSbBi alloys,[10] where it is described in detail. An example of the electronic band structure of $InP_{0.963}Bi_{0.037}$ obtained from DFT calculations is shown by thick curves in Fig. 3. It is clearly visible that the incorporation of Bi atoms into an InP host significantly modifies the band structure of InP. Bi-related changes are more distinct in Fig. 3(b) where the bands are plotted in the vicinity of the Γ point of the Brillouin zone. Figure 4 shows Bi-related changes in the position of the CB, heavy/light hole band, and the spin-orbit split off band obtained from *ab initio* calculations. These results clearly show that the band gap of InPBi narrows upon the incorporation of Bi atoms while the spin-orbit split-off significantly increases. The shift rates are,

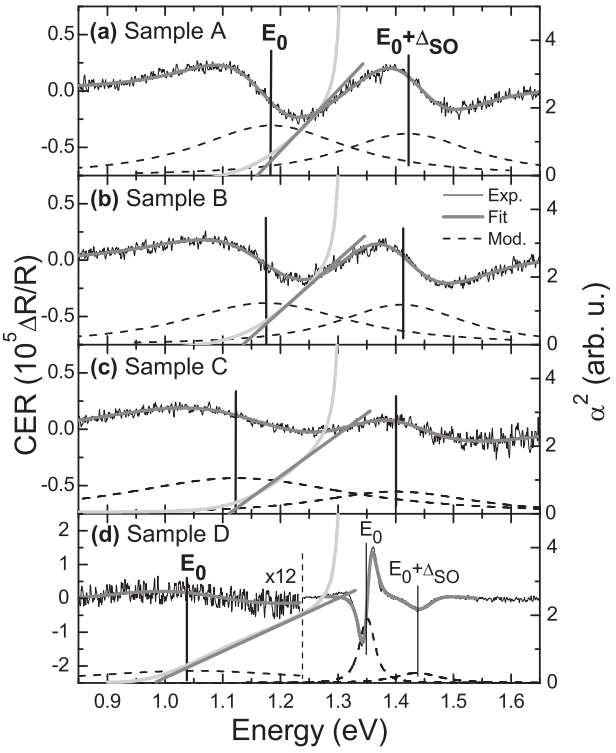

FIG. 1. Room temperature CER spectra of $InP_{1-x}Bi_x$ layers with various Bi concentrations together with the fitting curves (thick grey lines) and the moduli of CER resonance (dashed lines). Grey lines are absorption curves obtained at room temperature.

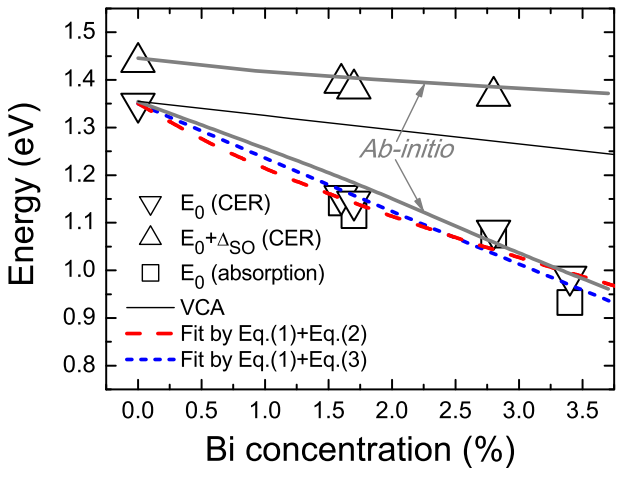

FIG. 2. Energies of E_0 and $E_0 + \Delta_{SO}$ transitions in $InP_{1-x}Bi_x$ alloys extracted from room temperature CER measurements (open triangles) and absorption measurements (open squares), which are corrected by the strain related shift,[11] together with theoretical predictions of energies of E_0 and $E_0 + \Delta_{SO}$ transitions obtained within *ab-inito* calculations (grey lines) as well as the theoretical formula given by Eq. (1) with the band gap bowing given by Eqs. (2) and (3). Assuming that the incorporation of Bi atoms in this range of concentration does not change significantly the hydrostatic deformation potentials and elastic constants the strain related shift of E_0 (heavy hole in this case) and $E_0 + \Delta_{SO}$ transition is estimated to be $\delta E_0^{HH} \approx 5.5$ eV $f_\perp$ and $\delta(E_0 + \Delta_{SO}) \approx 5.3$ eV $f_\perp$, where $f_\perp$ is the perpendicular mismatch given in Table I.

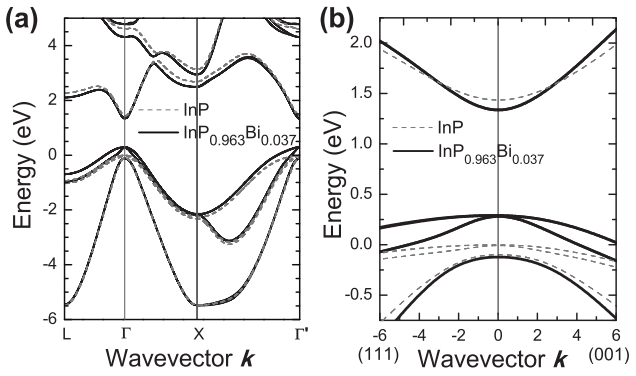

FIG. 3. Electronic band structure of $InP_{0.963}Bi_{0.037}$ (thick solid lines) calculated *ab initio* within the DFT together with the electronic band structure of InP host (grey dashed lines) at 0 K. L-Γ-X(-U)-Γ′ (Γ′ point from a neighbouring BZ) progression is presented.

respectively, −27 meV/% Bi for CB, 79 meV/% Bi for VB, and −7 meV/% Bi for the split-off band. These shifts of the conduction and valence band extrema give ∼75% (25%) valence (conduction) band offset between $InP_{1-x}Bi_x$ and InP. This means that the narrowing of the band gap is observed to be due to both the downward shift of the CB minimum and upward shift of the valence band (VB) maximum, while the enhancement of spin-orbit splitting is caused mainly by a strong shift of the heavy/light hole VB maximum towards the CB and only a very weak shift of the spin-orbit split off band.

The results of *ab initio* calculations are also plotted in Fig. 2 for comparison with experimental data. In order to match experimental data obtained at room temperature with the *ab initio* calculations, which corresponds to 0 K, energies of E_0 and $E_0 + \Delta_{SO}$ transitions obtained from *ab initio* calculations are shifted by −70 meV, i.e., a bandgap shift which is observed for these samples in absorption spectra in the 4–295 K temperature range.

Analyzing Fig. 2 we can conclude that the qualitative agreement between the DFT calculated energies of E_0 and $E_0 + \Delta_{SO}$ transitions and the experimental values is very satisfactory, i.e., the $E_0 + \Delta_{SO}$ transition redshifts with the increase in Bi concentration much less than the E_0 transition.

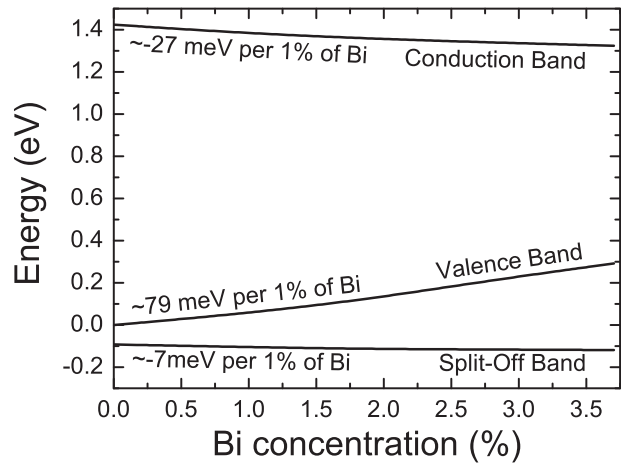

FIG. 4. Bi-related shifts of CB, VB, and spin-orbit split-off band in $InP_{1-x}Bi_x$.

However, the quantitative agreement between experimental data and theoretical calculations is less satisfactory. There are at least two factors, which lead to such a situation. The first is the built-in compressive strain in InPBi layers, which opens the band gap (i.e., leads to an increase in the energies of the E_0 and $E_0 + \Delta_{SO}$ transitions) and the second is the Bi content of InPBi layers. While the first factor can be easily included in our analysis (see, for example, Ref. 11 and details in the figure caption), the second factor is more complex. In order to determine the Bi concentration in the InPBi layers from XRD measurements, we have to know the lattice constant of zinc-blende InBi. This is somewhat controversial since InBi crystallizes in the tetragonal PbO-type structure rather than the cubic zinc-blende structure.[7,12] After previous studies[7] we assume that the lattice constant of InBi is 6.52 Å since this value is consistent with studies reported in Ref. 1 and leads to Bi concentrations which are close to those obtained from RBS studies. On the other hand, it is well known that any fraction of the atoms in highly mismatched alloys (in this case Bi atoms in InP host) that is not substitutional strongly affects the XRD results and analysis. The ionic radius of Bi is very similar to the ionic radius of In (1.17 vs. 0.94 Å for 3^+ ionic charge; note that the ionic radius of P is 0.58 Å (Ref. 13)) and hence some Bi atoms may occupy In sides. This can explain the difference between Bi concentrations determined from XRD and RBS studies for these samples. Moreover, it is very probable that Bi pairs or other clusters can be formed in InPBi similarly as in GaAsBi.[14] Taking into account experimental errors, the accuracy of *ab inito* calculations and above discussion we can summarize that the agreement between experimental data and theoretical predictions is acceptable for the early stages of investigation of this alloy.

The Bi-related variation of InPBi band gap can be modeled by a combination of the VCA with the VBAC model according to

$$E_g^{InP_{1-x}Bi_x} = (1-x)E_g^{InP} + xE_g^{InP} - \Delta E_g, \qquad (1)$$

where E_g^{InP} and E_g^{InBi} are the band gaps of InP and InBi, respectively. The ΔE_g is the band gap bowing, which can be calculated within the VBAC using

$$\Delta E_g = \frac{1}{2}\left(\sqrt{\Delta E_{Bi}{}^2 + 4C_{BiM}{}^2 x} - \Delta E_{Bi}\right), \qquad (2)$$

where ΔE_{Bi} is the energy distance from the Bi-level to the maximum of the VB, C_{BiM} is a constant, which describes the magnitude of interaction between Bi-related levels and VB states in InP, and x is a mole fraction of substitutional Bi atoms.

In order to determine the VBAC parameters for $InP_{1-x}Bi_x$, CER results have been fitted by Eq. (1) with the band gap bowing given by Eq. (2). The fitted curve is shown by dashed red line in Fig. 2. The magnitude of interaction between Bi-related levels and VB states in InP has been determined from this fit to be $C_{BiM} = 1.9 \pm 0.2$ eV. In this fit, the ΔE_{Bi} was fixed to be 0.23 eV. This value of ΔE_{Bi} results from the assumption that the Bi level lies at the same energy (on an absolute scale) for GaP and InP,[4] the VB offset between GaP and InP is 0.33 eV,[15] and that the Bi-level in

GaP is located 0.1 eV above the VB maximum.[16] In a first approximation, such estimation of the Bi-level in III-V host (i.e., the value of ΔE_{Bi}) can be accepted in the regime of dilute Bi concentrations similar as the estimation of N level in dilute nitrides.[17]

The other formula, which is typically used to describe the band gap bowing, is given by

$$\Delta E_g = bx(1-x), \tag{3}$$

where b is the bowing parameter and x is the alloy content. A fit of CER data with the band gap bowing given by Eq. (3) is shown by a short dashed blue line in Fig. 2. The bowing parameter determined from this fit equals 8.5 ± 0.5 eV. Such a large bowing parameter is unusual for regular III-V alloys,[15] but is typical for highly mismatched alloys which can be described within the BAC model.

In conclusion, applying CER spectroscopy to $InP_{1-x}Bi_x$ alloys with $0 < x \leq 0.034$ it has been determined that the E_0 transition shifts to longer wavelengths very significantly ($\sim$83 meV/% Bi), while the $E_0 + \Delta_{SO}$ transition red shifts very weakly ($\sim$13 meV/% Bi) with increasing Bi concentration. From the *ab initio* calculations, it has been determined that the incorporation of Bi atoms into an InP host modifies both the conduction and valence band. The shifts found in this work are, respectively, -27 meV per % Bi for CB and 79 meV per % Bi for the VB which leads to a band gap reduction of 106 meV per % Bi. The obtained DFT results are very consistent with the experimental data.

The authors acknowledge financial support from the NCN Poland (Grant No. EP/G004447/2). K. W., Y. G., Q. G. and S. W. would like to acknowledge the financial support from the National Basic Research Program of China (Grant No. 2014CB643902) and the Natural Science Foundation of China (Grant No. 61334004 and No. 61404152). M.P.P. acknowledges for support within the "Diamond Grant" (DI2013 006143) from the MNiSzW. The *ab initio* calculations were performed in the WCNS.

[1]K. Oe and H. Okamoto, Jpn. J. Appl. Phys., Part 2 **37**, L1283 (1998).
[2]B. Fluegel, S. Francoeur, A. Mascarenhas, S. Tixier, E. C. Young, and T. Tiedje, Phys. Rev. Lett. **97**, 067205 (2006).
[3]K. Bertulis, A. Krotkus, G. Aleksejenko, V. Pacebutas, R. Adomavicius, G. Molis, and S. Marcinkevicius, Appl. Phys. Lett. **88**, 201112 (2006).
[4]K. Alberi, J. Wu, W. Walukiewicz, K. M. Yu, O. D. Dubon, S. P. Watkins, C. X. Wang, X. Liu, Y.-J. Cho, and J. Furdyna, Phys. Rev. B **75**, 045203 (2007).
[5]R. Kudrawiec, J. Kopaczek, J. Misiewicz, J. P. Petropoulos, Y. Zhong, and J. M. O. Zide, Appl. Phys. Lett. **99**, 251906 (2011).
[6]Y. Gu, K. Wang, H. Zhou, Y. Li, C. Cao, L. Zhang, Y. Zhang, Q. Gong, and S. Wang, Nanoscale Res. Lett. **9**, 24 (2014).
[7]K. Wang, Y. Gu, H. F. Zhou, L. Y. Zhang, C. Z. Kang, M. J. Wu, W. W. Pan, P. F. Lu, Q. Gong, and S. M. Wang, Sci. Rep. **4**, 5449 (2014).
[8]R. Kudrawiec, Phys. Status Solidi B **247**, 1616 (2010).
[9]A. Janotti, S.-H. Wei, and S. B. Zhang, Phys. Rev. B **65**, 115203 (2002).
[10]M. P. Polak, P. Scharoch, R. Kudrawiec, J. Kopaczek, M. J. Winiarski, W. M. Linhart, M. K. Rajpalke, K. M. Yu, T. S. Jones, M. J. Ashwin, and T. D. Veal, J. Phys. D: Appl. Phys. **47**, 355107 (2014).
[11]M. Welna, R. Kudrawiec, Y. Nabetani, and W. Walukiewicz, Appl. Phys. Express **7**, 071202 (2014).
[12]M. Ferhat and A. Zaoui, Phys. Rev. B **73**, 115107 (2006).
[13]R. D. Shannon, Acta Crystallogr., Sect. **A32**, 751 (1976).
[14]G. Ciatto, E. C. Young, F. Glas, J. Chen, R. Alonso Mori, and T. Tiedje, Phys. Rev. B **78**, 035325 (2008).
[15]I. Vurgaftman, J. R. Meyer, and L. R. Ram-Mohan, J. Appl. Phys. **89**, 5815 (2001).
[16]F. A. Trumbore, M. Gershenzon, and D. G. Thomas, Appl. Phys. Lett. **9**, 4 (1966).
[17]G. Pettinari, M. Felici, R. Tarotta, M. Capizzi, and A. Polimeni, J. Appl. Phys. **115**, 012011 (2014).